Volumetric behavior of saturated sands under poor drainage conditions

Sérgio D. N. Lourenço,[1,2] Gonghui Wang,[3] Kyoji Sassa,[3] and Hiroshi Fukuoka[3]

Received 8 April 2005; revised 17 March 2006; accepted 3 April 2006; published 15 July 2006.

[1] Permeability variations have been identified as a key factor in controlling slope failure locations in rainfall-induced landslides. In this research, failure behavior in limited drainage conditions was investigated. Tests were performed on saturated sands by means of a modified triaxial system that could mimic the effect of low-permeability barriers present in the field. The tests were conducted by increasing the pore water pressure at different rates to study the effects of the speed of pore water pressure rise on soil failure. The results revealed a dependence of soil volume changes on the rate of pore water pressure increase. In general, the results showed that volume change of granular soils, which are under shear and confined laterally by low-permeability materials, depends on the initial porosity and the pore water pressure rate. These results are particularly valid during the early stages of soil deformation that precede wholesale slope failure.

Citation: Lourenço, S. D. N., G. Wang, K. Sassa, and H. Fukuoka (2006), Volumetric behavior of saturated sands under poor drainage conditions, *J. Geophys. Res.*, *111*, F03004, doi:10.1029/2005JF000324.

1. Introduction

[2] Excess pore water pressure (pore water pressure in excess of hydrostatic pressure) has been identified as a slope failure trigger under different initial conditions and scales.

[3] 1. *Harp et al.* [1990], *Bonte et al.* [2000], and *Ochiai et al.* [2004] recorded excess pore water pressures during induced failures in natural slopes. *McDonnell* [1990] and *Johnson and Sitar* [1990] also measured high pore water pressure generation in the vicinity of failures triggered by heavy rainfall.

[4] 2. Slope failures have also been triggered by an increase of pore water pressure in laboratory experiments performed at different scales and under different configurations and initial conditions. *Eckersley* [1986, 1990] obtained a flow failure by slowly raising the water table level in a coal stockpile; *Iverson et al.* [1997, 2000], *Reid et al.* [2000], and *Moriwaki et al.* [2004] triggered failures under different hydrologic conditions (infiltration intensities and directions) and initial porosities. *Wang and Sassa* [2001, 2003] also measured positive excess pore water pressure before and during failure in small-scale flume tests.

[5] Because of the heterogeneous nature of most soils it is likely that excess pore water pressures during infiltration in natural slopes develop within layers of high permeability surrounded by low-permeability materials [*Reid*, 1995; *Vieira and Fernandes*, 2004]. These porosity and grain size variations act as physical barriers to groundwater flow, creating high pore water pressure gradients and endangering slope stability. In fact, *Reid* [1995] demonstrated that slight variations of permeability (10X) are enough for perched groundwater to occur. Low-permeability bedrock and impermeable geological structures can also provide the necessary trapping conditions.

[6] We hypothesize that if a potential shear surface is confined by low-permeability materials, the rate of pore water pressure increase could influence the volumetric response during failure. For example, if water is unable to flow in a hypothetical shear surface due to the presence of an impermeable material, the pore water pressure increase rate (henceforth, PPIR) will affect the volumetric response by modifying the tendency of the soil for dilation or contraction while the soil is under shear. Figure 1 illustrates porosity and fine particle variations that could affect groundwater flow. These porosity and fine particle variations (i.e., permeability variations) can dictate the shear surface location. In Figure 1, position 1 corresponds to a location where groundwater could circulate freely, whereas in position 2, groundwater flow would be impeded and high with pore water pressures would be generated. In this paper we investigate landslide behavior in situations resembling position 2.

[7] The approach of our research was to investigate experimentally, by triaxial testing, the role of drainage on the volumetric behavior of saturated sands and its relation with rainfall-induced landslides. We focused on the behavior of soils subjected to limited drainage conditions.

2. Volumetric Behavior and Failure Mode

[8] When a soil specimen is sheared in a triaxial cell, the volumetric response of the soil might follow two different paths: contraction (volume decrease) or dilation (volume increase). Soil contracts if the porosity at large strains is

[1]School of Engineering, Durham University, Durham, UK.
[2]Formerly at Disaster Prevention Research Institute, Kyoto University, Kyoto, Japan.
[3]Disaster Prevention Research Institute, Kyoto University, Kyoto, Japan.

0148-0227/06/2005JF000324

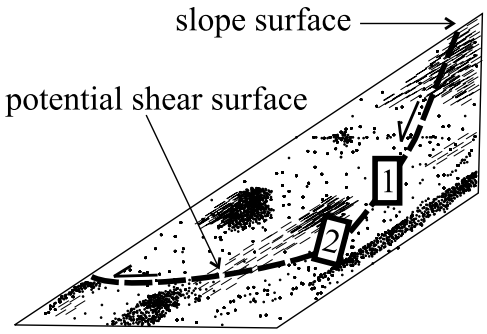

Figure 1. Schematic illustration of rainfall-induced failure in heterogeneous soil. Simulation of shear behavior is shown in positions 1 and 2. The shear surface is confined in position 2. Texture concentration illustrates porosity variations. Dots represent sandy soil; dashes denote clayey soils.

smaller than the initial porosity and dilates if porosity in large strains is larger than the initial porosity. Loose and dense sands at the same confining pressure approach the same porosity (the void ratio corresponding to this porosity is called critical void ratio) when sheared to large strains [*Casagrande*, 1936]. Constant porosities at large strains impose a steady state of deformation; this is the state in which a mass of particles continuously deforms at constant volume, constant shear stress and constant velocity [*Poulos*, 1981]. The volumetric behavior in a triaxial test is defined by the ratio of the volumetric strain (ε_v) to the axial strain (ε_a) in drained conditions. This ratio is positive for dilation of the soil and negative for contraction.

[9] The probability of a specimen contracting or dilating during shear will depend on (1) the initial conditions (initial porosity, initial stresses, specimen preparation method), (2) the boundary drainage conditions, (3) the way the principal stresses σ_1 and σ_3 vary during shear, and (4) the rate of change of σ_1 and σ_3. For example, contraction of a saturated specimen in loose state will depend on the imposed drainage conditions and the rate of shear stress change. Such contraction can result in a sudden buildup of pore water pressure at small strains together with a fast increase of the axial strain, i.e., the specimen collapses instantly.

[10] The soil volumetric behavior in a triaxial test can be associated with a particular failure mode in the field. Contraction of saturated soil in a loose state indicates liquefaction or flow failure, which has been widely demonstrated in both experimental tests and in the field [*Castro*, 1969; *Eckersley*, 1986, 1990; *Iverson*, 1997; *Iverson et al.*, 1997, 2000]. On the other hand, dilation is compatible with a slide which might mobilize to a flow or move slowly down the slope [*Ellen and Fleming*, 1987]. *Iverson et al.* [2000] recorded repetitive stop-advance movements in landslide experiments performed with dense sands, with pore water pressure dropping during shear as the soil dilated and rising when the soil was at rest.

[11] The soil may also be subjected to volumetric changes prior to failure. A volume decrease, in the form of surface settlement, has been recorded in two-dimensional physical tests. *Wang and Sassa* [2001, 2003] and *Eckersley* [1986, 1990] monitored a surface settlement during the water table rise of loose granular soils. In these circumstances, the pore water pressure buildup might have been accelerated by the decreasing volume of the soil. In triaxial tests, a loose granular specimen often decreases its volume during saturation. In the field, the monitoring of rainfall-induced failures has focused on measuring the soil displacement parallel to the slope, and not in the vertical direction. Consequently, there is no strong evidence of surface settlement before failure in the field. *Ochiai et al.* [2004] and *Moriwaki et al.* [2004], for example, recorded increasing deformations in a rainfall-induced failure on a natural slope, but unfortunately it is not possible to infer whether the deformations were contributing to a volume reduction or not. Dense soils are not subject to volumetric changes during water table rise.

[12] In the tests reported in this paper, the PPIR is a surrogate for the speed of a water table rise in the soil. In natural slopes, factors contributing to the water table rise include (1) rainfall, (2) water flow from pipes (*McDonnell* [1990] has shown that pipe flow can contribute significantly on the formation of perched water tables), and (3) lateral infiltration from the bedrock (*Johnson and Sitar* [1990] identified lateral infiltrations from permeable bedrock). These different sources affect the PPIR.

3. Testing Approach

[13] Triaxial testing is a common laboratory technique used in soil mechanics to determine the strength parameters of soils (cohesion and friction angle). It allows carrying out experiments with fully controlled stresses, volume changes, pore water pressures and drainage conditions. Several studies conducted in the triaxial apparatus have improved the knowledge of slope failures: liquefaction, for example, which results in flow-type failure in the field, was first identified in the laboratory by triaxial undrained tests on very loose sands [*Castro*, 1969]. Such small-scale testing is therefore a plausible way of studying landslide behavior, especially initial failure.

[14] Our triaxial testing program emphasized two conditions: (1) water must be able to flow through the specimen and failure must be controlled exclusively by pore water pressure; (2) the drainage conditions should also be controlled and should include a low-permeability barrier to decrease drainage to the exterior. Condition (1) was satisfied by performing Constant Shear Stress Drained triaxial tests [e.g., *Anderson and Sitar*, 1995; *Zhu and Anderson*, 1998; *Anderson and Riemer*, 1995; *Chen and Yang*, 2000; *Chu et al.*, 2003]. These are pore water pressure-controlled tests. The goal is to ensure that shearing of the soil is controlled by pore water pressure, only. This testing procedure mimics the natural slope process realistically, by decreasing the soil strength through an increase of pore water pressure [*Brand*, 1981; *Bishop and Henkel*, 1964].

[15] Condition (2) was addressed by decreasing the permeability of one extremity of the soil specimens, thereby simulating a surrounding low-conductivity material. This could be achieved by decreasing the drainage potential of the apparatus itself (henceforth ''equivalent permeability'') to a value less than the specimen's own permeability, inducing a partially drained condition to the specimen.

[16] Specimens consisted of fine-grained silica sand #7 (SS#7) and Toyoura sand (TS). SS#7 is an industrial sand

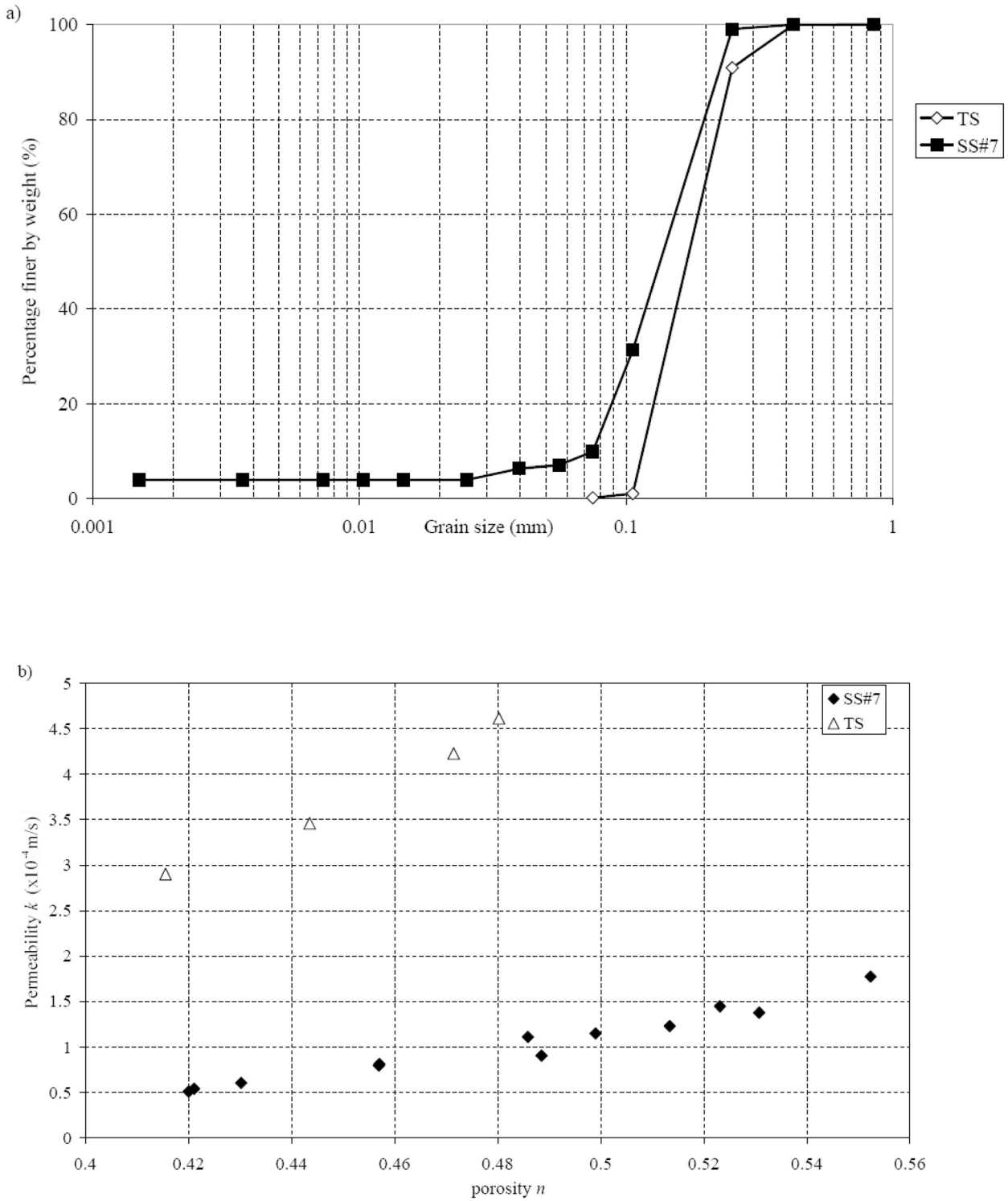

Figure 2. (a) Grain size distribution curves for silica sand #7 (SS#7) and Toyoura sand (TS). (b) Variation of permeability versus void ratio ($k = 0.13 + 0.196e^3/(1 + e)$, $e = n/(1 - n)$, correlation coefficient $R = 0.98$ for SS#7; $k = 0.885 + 9.06*e^3/(1 + e)$, $e = n/(1 - n)$, correlation coefficient $R = 0.97$ for TS).

with subangular grains with a mean grain size of 0.13 mm, and uniformity coefficient of 2.10. TS is a standard sand of the Japanese Geotechnical Society, composed of sub-rounded grains with mean grain size of 0.11 mm and uniformity coefficient of 1.6. The grain size distributions of SS#7 and TS are shown in Figure 2a. Note that those grains smaller than 0.005 mm existing in SS#7 could be classified as fine silt or rock flour, because they are formed

Table 1. Soil Properties

Physical Parameters	Symbol (Units)	Soil	
		Silica Sand #7	Toyoura Sand
Mean grain size	D_{50} (mm)	0.13	0.17
Effective grain size	D_{10} (mm)	0.074	0.11
Uniformity coefficient	U_c	2.10	1.60
Maximum porosity	n_{max}	0.55	0.50
Minimum porosity	n_{min}	0.41	0.38
Specific gravity	G_s	2.63	2.64
Internal friction angle[a]	ϕ' (degrees)	35.19	31.70

[a]For loose conditions.

by mechanical grinding. Figure 2b plots the permeability of SS#7 and TS against void ratio. The variation of permeability was estimated (not measured) and is given as a regression function of void ratio fitted to the Kozeny-Carman equation [*Mitchell*, 1993]. Some other properties of these specimens are listed in Table 1.

[17] The drainage potential of the triaxial apparatus (taking into account the porous plate, the pipe connecting the specimen to the exterior, and the filter paper) was measured to have an overall equivalent permeability of 7×10^{-6} m/s, two orders smaller than those of SS#7 and TS (Figure 3). Note that the equivalent permeability of the apparatus was obtained from the bottom part. However, because the upper part is structured identically to the bottom part, an equal equivalent permeability is expected and used in the analysis of the data. Tests 1, 2, 4, 6, 8, 10 were performed by upward infiltration, and tests 3, 5, 7, 9, 11, 12, 13, and 14 by downward infiltration.

4. Testing Program and Procedure

[18] To examine the effects of the PPIR, initially 4 tests (tests 1, 2, 4, and 6 in Table 2) were prepared with the same initial conditions (specimen of TS, nearly identical porosity and σ_3/σ_1) but performed at different PPIRs for loose specimens (prepared by dry deposition). Another 4 tests (tests 7–10) with dense specimens were performed at three different PPIRs. These dense specimens were prepared by dry tamping and consolidated at two different values of σ_3/σ_1, i.e., the specimens were anisotropically consolidated. Tests 3 and 5 were performed on SS#7 at different values of σ_3/σ_1. In tests 11 to 14, the specimens of SS#7 were prepared at different initial porosities, but the tests were conducted with similar PPIRs. All the specimens had a volume of approximately 1550 cm^3 (20cm height and 10cm diameter). Tests were performed at the lowest possible confining pressure: 50 kPa. This was the lowest possible value at which results could accurately be recorded.

[19] To define the lowest PPIR for the testing program, preliminary tests conducted at 0.0018 kPa/s and 0.018 kPa/s revealed very similar results, suggesting that 0.0018 kPa/s would be an acceptable minimum rate. Most of the tests were performed with higher PPIR values of 0.14–0.18 kPa/s and 0.012–0.014 kPa/s. Note that only test 2 was performed with a PPIR of 0.0018 kPa/s. The testing program is summarized in Table 2.

[20] To perform each test, a rubber membrane of 0.2mm thickness was first set on the pedestal of the apparatus, and then the soil was poured rapidly into the mould by dry deposition to get the loosest possible condition, and dry tamping was used to get dense specimens. After this, a vacuum pressure (−15 kPa) was applied so that the specimen could stand by itself. The cell chamber was filled with water and an initial confining pressure of 15 kPa applied while the atmospheric air pressure in the specimen was restored. After 2 hours of CO_2 circulation, the specimen was filled with de-aired water. The de-aired water was left to circulate for 8 hours and then in order to ensure a high degree of saturation with a pore water pressure coefficient, B [*Bishop and Henkel*, 1964], approximately equal to 1 backpressure was applied in steps to a maximum of 150 kPa. While increasing the backpressure, the effective stress decreased (to ensure full saturation) until a very small value of 5 kPa was reached. In this way a B value of approximately 1 was easily obtained for every loose specimen. For dense specimens the B value was approximately 0.96. After checking the degree of saturation at 50 kPa, σ_1 was increased slowly (at a rate of 0.1 kPa/s) in a drained condition until the desired value of σ_3/σ_1. Finally, the test started by increasing the pore water pressure through the top or bottom of the specimen at a desired rate, while the vertical stress and confining pressure were held constant.

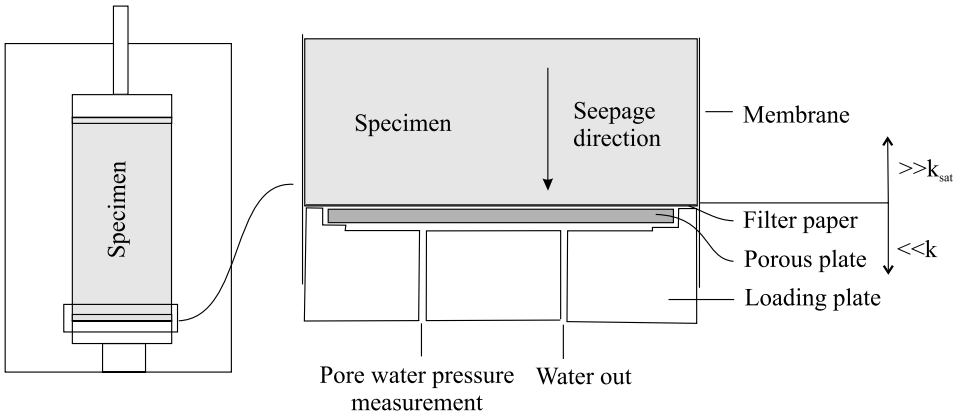

Figure 3. Details of the apparatus arrangement in order to simulate slope failures under limited drainage conditions. Water enters through the top or bottom of the specimen and percolates through it at a controlled pore water pressure rate; when it reaches the bottom end or the upper end, the porous plate will decrease the water discharge to the exterior, acting as a barrier to water flow.

Table 2. Laboratory Testing Program[a]

Parameters	Symbol (Units)	Tests													
		1	2	3	4	5	6	7	8	9	10	11	12	13	14
Soil		TS	TS	SS#7	TS	SS#7	TS	TS	TS	TS	TS	SS#7	SS#7	SS#7	SS#7
Deposition method		DD	DD	DD	DD	DD	DD	DT	DT	DT	DT	DD	DT	DT	DT
Initial state of stress	σ_3/σ_1	0.30	0.30	0.35	0.30	0.35	0.30	0.5	0.30	0.50	0.30	0.50	0.50	0.50	0.50
Initial porosity	n	0.49	0.49	0.52	0.49	0.52	0.48	0.40	0.40	0.42	0.41	0.52	0.49	0.46	0.44
PPIR[b]	$\delta u/\delta t$ (kPa/s)	0.018	0.0018	0.013	0.16	0.14	0.33	0.014	0.014	0.14	0.15	0.013	0.013	0.013	0.013

[a]DD, dry deposition; DT, dry tamping; TS, Toyoura; SS#7, silica sand #7.
[b]Pore water pressure increase rate.

[21] The testing arrangement and operating system is illustrated in Figure 4. As shown, the pore water pressure transducers were located externally, not directly in contact with the specimen. Volume changes of soil specimens were measured indirectly by means of a differential pressure transducer connected to the cell chamber. It is worth noting here that the effect of the moving piston inside the cell chamber on the measured volume change was subtracted through the accurate measurement of vertical displacement. However, the possible effect of membrane penetration and deformation was not considered due to the following reasons. (1) The applied confining pressure was small (50 kPa). (2) The deposition of the fine-grained loose sand in the mould resulted in a homogeneous structure and uniformly distributed voids between sand particles at the soil-membrane interface (therefore any membrane penetration effect was discounted). (3) During the test the confining pressure was always greater than the pore water pressure applied to the specimen, so there should not be any separation of the membrane from the specimen. (4) Changes in the elastic deformation of the membrane were very small, because the increasing pore water pressure only reduced the effective stress within the specimen, and did not affect the confining pressure on the membrane.

5. Results

5.1. Failure Behavior

[22] Because of the imposed testing conditions, the only variables varying freely during the tests were the axial displacement and specimen volume change. In every test, specimens exhibited a dilatant behavior, regardless of the PPIRs and imposed initial conditions. No tendency for contraction was observed.

[23] To exemplify the failure behavior, results of three tests (tests 5, 7, and 11) are presented in Figures 5, 6, and 7, respectively. Figures 5a, 6a, and 7a illustrate the time series data for stresses (σ_1, σ_3) and pore water pressures. In Figure 5a it can be seen that the pore water pressure dropped slightly and then recovered in response to soil dilation after the onset of failure. This phenomenon can also been seen in Figures 6a and 7a.

[24] The results show that the total stresses remained constant throughout the test while the pore water pressure was increased. The pore water pressure increased until it produced the smallest amount of effective confining stress under which the soil could sustain the constant deviatoric stress. Figures 5a, 6a, and 7a show that after failure there was a slight drop (approximately 10%) of the vertical stress, probably due to the fact that the piston was unable to follow the fast shearing speed of the soil.

[25] The volumetric strain (ε_v), axial strain (ε_a), and the acceleration curve (derived from the axial displacement) for the three tests are presented in Figures 5b, 6b, and 7b. The deformation onset was identified based on the specimen's volumetric changes and vertical displacement. The failure onset was determined by the point of maximum curvature of the acceleration curve. As soon as the deforming soil reaches this point, the specimen will inevitably fail with

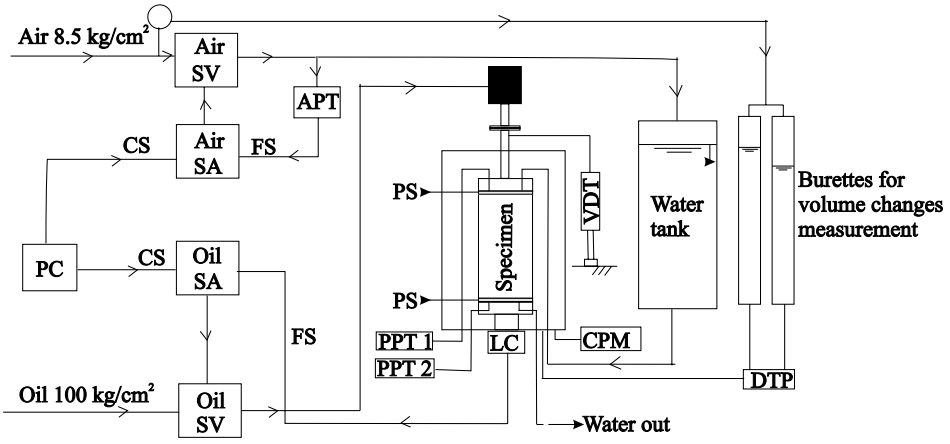

LEGEND: SV=servo-valve; SA=servoamplifyer; CS=command signal; FS=feedback signal;
CPM=cell pressure meter; DTP=duplex tube burette; DPT=differential pressure transducer; LC=load cell;
VDT= vertical displacement transducer; PPT= pore pressure transducer; PS=Porous Stone;
APT=air pressure transducer

Figure 4. Operating and measurement system.

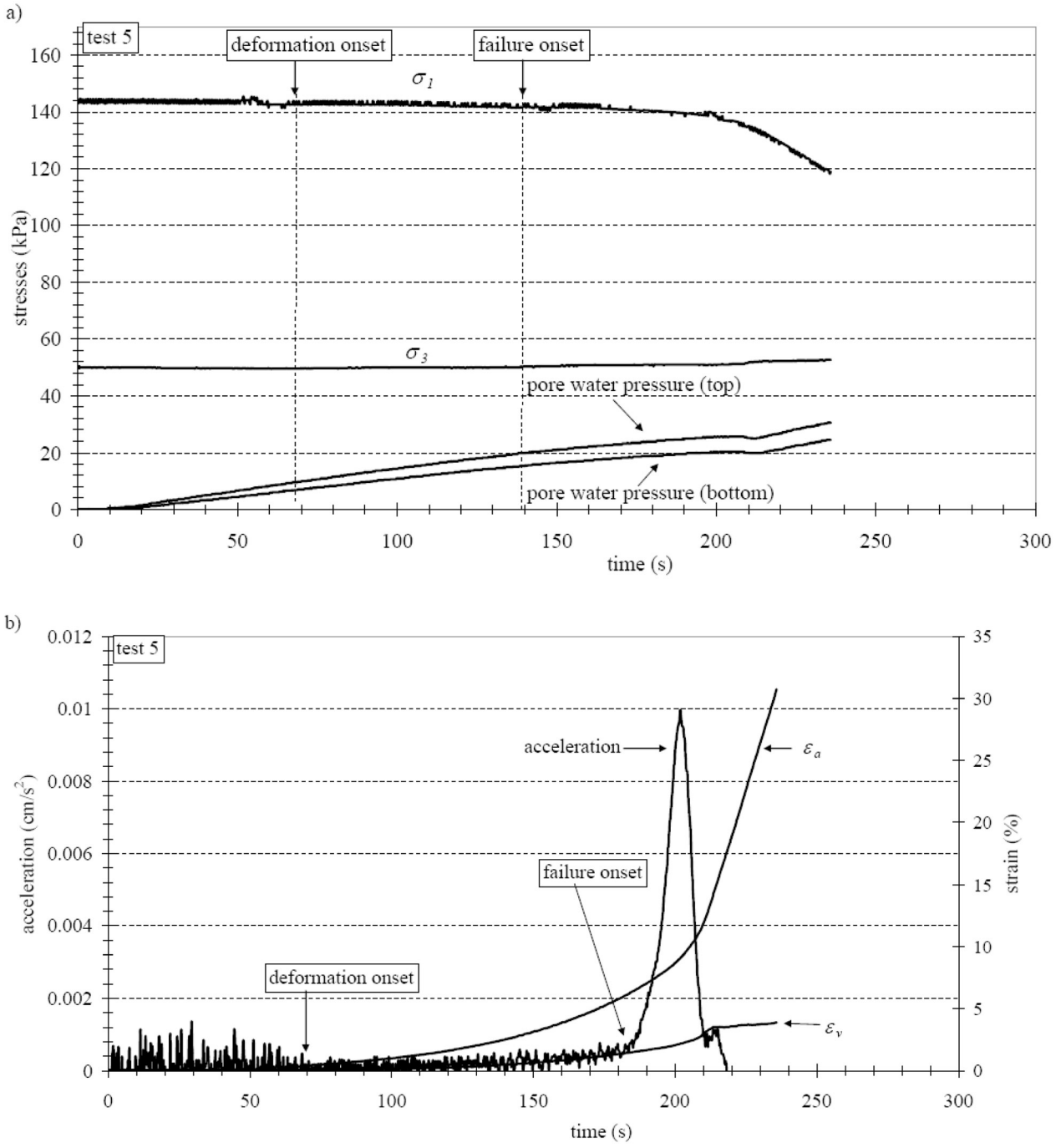

Figure 5. Time series data for test 5. (a) Vertical stress (σ_1), cell pressure (σ_3), and pore water pressure (top and bottom); (b) acceleration, volumetric strain (ε_v), and axial strain (ε_a).

no possible return to stability. The acceleration curve reaches a peak and then decreases. The decrease can coincide with the decrease of the deviatoric stress (as shown in Figure 6a, for example). The results also revealed that no volumetric variations occurred before the deformation onset, although the pore water pressure had increased substantially (Figures 5b, 6b, and 7b); this trend is consistent with those obtained in similar tests performed by other authors [e.g., *Chu et al.*, 2003].

5.2. Effect of Pore Water Pressure Increase Rate

[26] The results indicate that the effect of the PPIR on the volumetric response of the soil under restricted drainage conditions was significant. Figures 8 and 9 show the results of 10 tests performed on different specimens at different PPIRs. Figures 8 and 9 depict the ratio between ε_v and ε_a as specimens underwent shear. Failure onset is marked with a circle for each test. Figure 8 illustrates the results for tests 1 to 6. The results clearly show the effect of PPIR on the

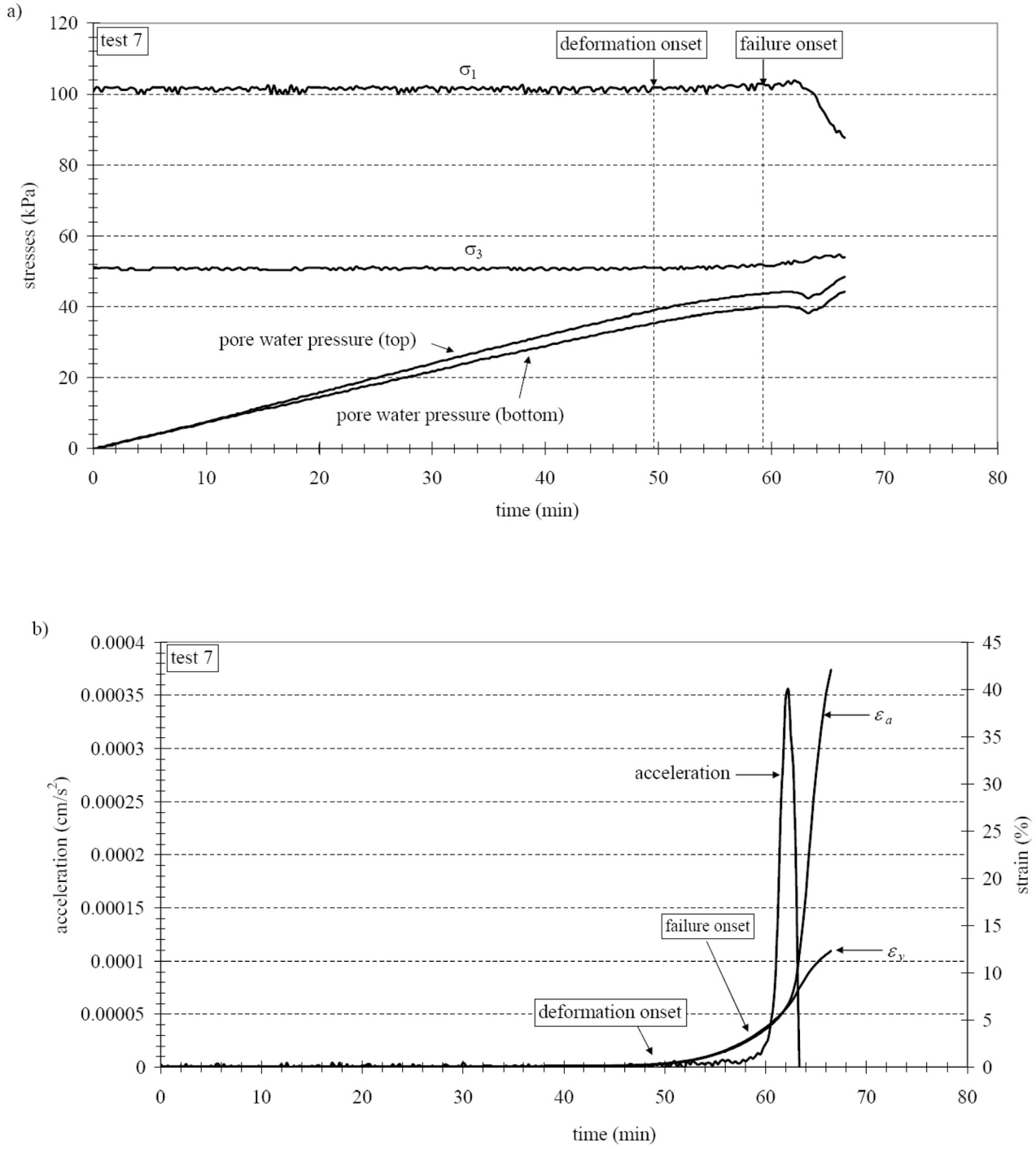

Figure 6. Time series data for test 7. (a) Vertical stress (σ_1), cell pressure (σ_3), and pore water pressure (top and bottom); b) acceleration, volumetric strain (ε_v), and axial strain (ε_a).

specimen volumetric variations. For tests 3 and 5 (performed on loose SS#7), an increase of PPIR from 0.013 to 0.14 kPa/s resulted in an increase of ε_v from 2.2% to 3.6% at the axial strain (ε_a) of 20%. Similar trends can also be observed from tests 4 and 6 performed on loose TS, where ε_v increased from 2.93% to 5.47%. Note that the cyclic behavior recorded in test 3 was not intentionally induced; this phenomenon may be attributed to cycles of dilation-contraction when ε_a was continuously increasing.

[27] By comparing Figure 8 to Figure 9, the following observations can be made.

[28] 1. The dense specimens exhibited greater volumetric expansion compared to the loose specimens, their volumetric strain (ε_v) ranged approximately between 10 and 16%, while the loose specimens between 1.6 and 3.6% (if discounting test 6 which was the only one performed at 0.3 kPa/s). This difference can be explained by the lower porosity of the dense specimens. Consequently, it can be

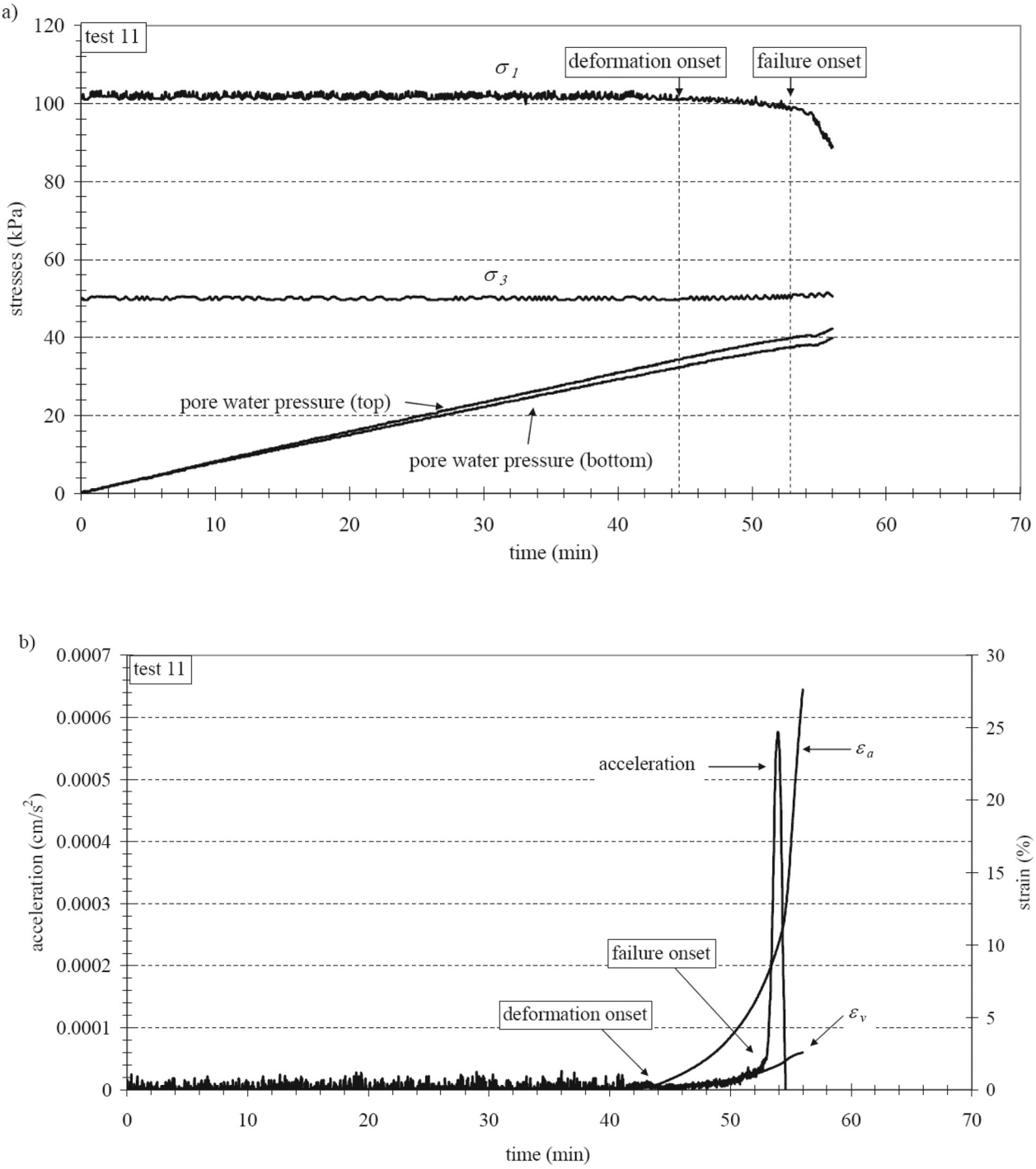

Figure 7. Time series data for test 11. (a) Vertical stress (σ_1), cell pressure (σ_3), and pore water pressure (top and bottom); (b) acceleration, volumetric strain (ε_v), and axial strain (ε_a).

assumed that specimens consolidated to lower initial porosities undergo increasing volumetric strains for the same PPIR, as observed in Figure 10 (the volumetric strain corresponding to the axial strain of 18% is plotted against the PPIR for loose and dense specimens).

[29] 2. The loose specimens reached their steady states after a finite amount of axial strain (less than 20% in Figure 8). Afterward, the volumetric strain did not change further with increasing axial strain. However, for the dense specimens the volumetric strain was continuously increasing with axial strains up to 20%.

[30] 3. The slope of the curve $\varepsilon_v - \varepsilon_a$ became gentler with increasing ε_a.

[31] An additional set of pore water pressure controlled tests (tests 11–14) was performed by maintaining PPIR constant and varying the initial specimen porosities. The test

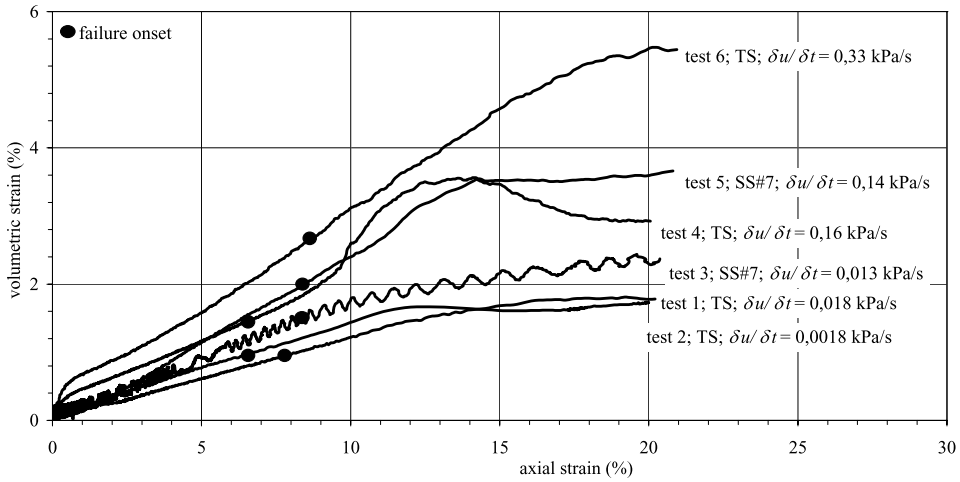

Figure 8. Volumetric response. Pore water pressure rate effect for loose specimens ($n \approx 0{,}50$).

results are presented in Figure 11 in the form of volumetric strain against axial strain. The goal was to compare the effect of the pore water pressure increase rate to that of the initial porosity. Results confirmed expectations with the specimens increasing their volume strain as the initial porosity decreased (Figure 11).

6. Discussion

6.1. Physical Interpretations

[32] The effect of the PPIR on soil dilation is analogous to the effect of the initial porosity: denser soils (smaller in porosity) have greater dilatant tendency throughout shearing, and the same is true for confined soils under a high PPIR. However, the physical mechanisms acting on the soil in both situations are different. For a dense soil under shear, dilation is simply due to arrays of grains overlapping each other; for confined soils this phenomenon can be enhanced by seepage force associated with the water flow conditions imposed on the soil, i.e., the soil tends to increase its volume even more due to flowing water.

[33] Shear in granular soils tends to be concentrated in shear bands [e.g., *Nemat-Nasser and Okada*, 2001]. In our experiments, the dense specimens exhibited clear shear bands, while the loose specimens developed a barrel-like shape with several minor shear bands. As the failure mode was mostly dependent on the initial porosity (no visible major changes occurred under the different testing conditions), all the dilation could have been concentrated in the shear bands. The increased volumetric strain could then be explained physically by an increase on the thickness of the shear band (with several arrays of grains under shear), and could involve a partial detachment of grains in the shear zone (but not a complete separation of grains as this could lead to a complete loss of strength).

[34] *Junaideen* [2005] performed 2 pore water pressure controlled tests at two different rates in sandy soils, and only a small increase of ε_v was measured. The author explained this behavior based on a slight difference of the initial porosity and not on the PPIR used. Other possible reasons for such difference include (1) the pore water pressure was increased by applying backpressure, with no water flow (the lack of water flowing out could have restrained the volumetric response of the soil) and (2) the rates used were slightly lower than our rates (0.0027 kPa/s and 0.0083 kPa/s), our tests suggest that there is a minimum rate for the volume increase to be observed.

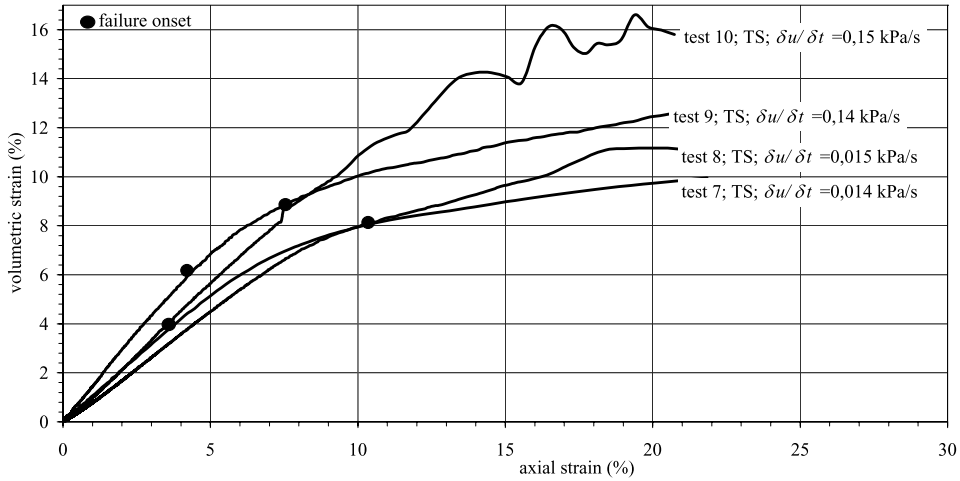

Figure 9. Volumetric response. Pore water pressure rate effect for dense specimens ($n \approx 0{,}41$).

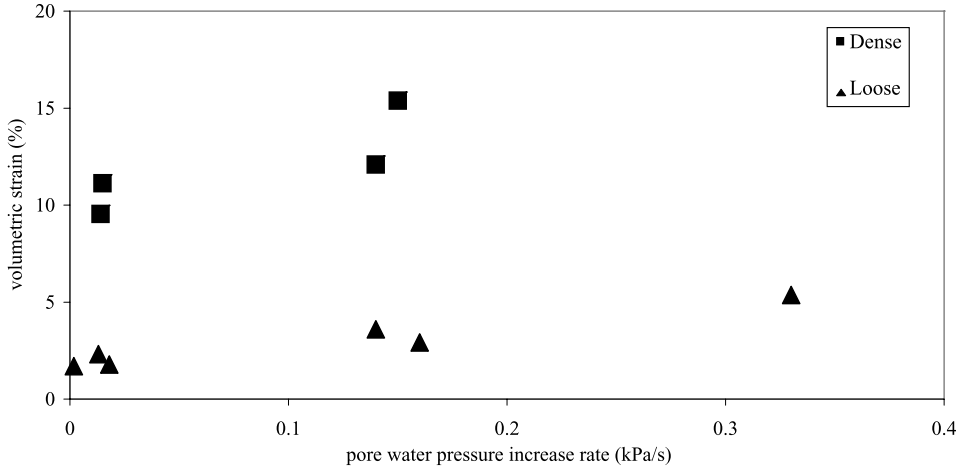

Figure 10. Pore water pressure rate versus volumetric strain at 18% of axial strain for the loose and dense specimens.

[35] The effect of PPIR at larger scales is unknown. Some landslides have been triggered in natural slopes or in laboratory model tests by sprinkling water or by infiltrating water from the bottom of the soil [*Eckersley*, 1990; *Iverson et al.*, 1997; *Reid et al.*, 2000; *Wang and Sassa*, 2001; *Moriwaki et al.*, 2004; *Ochiai et al.*, 2004; *Lourenço et al.*, 2006]. In these conditions, pore water pressure is a result of infiltration and volumetric changes. *Reid et al.* [2000] performed physical tests by varying the sprinkling intensity; the results revealed that pore water pressure was generated at the downslope end of the model for moderate-intensity sprinkling tests, while for the high-intensity sprinkling test pore water pressure was only generated during failure. As a result, changing the sprinkling intensity had no clear effect on the generated pore water pressure. Therefore evidence of the PPIR effect remains restricted to triaxial testing.

6.2. Implications for Rainfall-Induced Landslides

[36] In our testing procedure, the pore water pressure was controlled throughout the test, i.e., it was increasing before and during failure. However, this is unrealistic in natural slopes; the pore water pressure continuously increasing in a dilative soil is improbable; *Harp et al.* [1990] and *Ochiai et al.* [2004] recorded in rainfall-induced landslide experiments decreasing pore water pressures just before failure due to crack and pipe formation. Therefore application of these results to rainfall-induced landslides (particularly for dilative mobilizations) would require the occurrence of low-permeability barriers and would depend on the displacement attained by the soil mass. The results are mostly valid during prefailure deformation (before reaching the critical void ratio) of the soil and possibly during the early development of the shear surface, when it is possible that

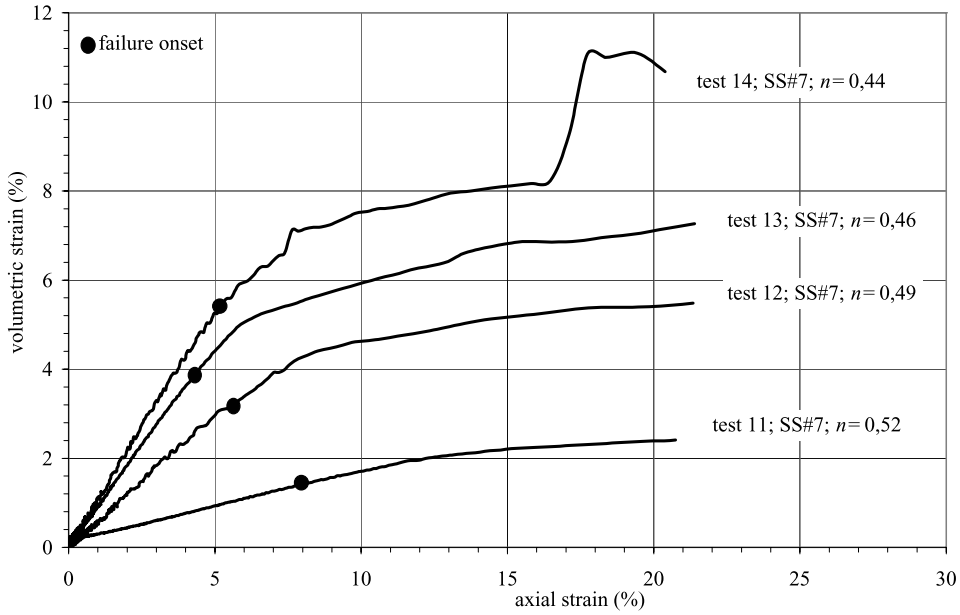

Figure 11. Volumetric response. Initial porosity effect is for the same pore water pressure rate (≈0,013 kPa/s).

the soil is deforming, the pore water pressure is rising, and the slope still holds its original heterogeneous structure (with all the permeability variations which affect the groundwater flow).

[37] For large displacements, it is unlikely that the initial structure is preserved and, therefore pore water pressure rate variations would have a minimal impact on the overall volumetric response of the soil. In these large strains it is more probable that the volumetric variations were being controlled by the temporal rates of slope deformation and pore water pressure variations [*Iverson et al.*, 1997].

[38] If pore water pressure can continuously increase during failure in a dilative soil in a natural slope (as in our tests), the increasing pore water pressure would enable the soil to dilate to a state looser than the usual critical state, which could induce a contractive response during failure and enhance the potential for high mobility of the landslide mass.

7. Conclusions

[39] Pore water pressure controlled tests were performed in anisotropically consolidated fine-grained sands in a triaxial system, where the specimens were brought to failure by increasing the pore water pressure inside the specimen while the shear stress was held constant. Several tests (10) were conducted for different PPIRs (ranging from 0.18 kPa/s to 0.012 kPa/s), and different initial porosities. The volumetric behavior was studied by the ratio of the ε_v against ε_a.

[40] The results clearly showed a dependence of the soil dilation on the PPIR, with the magnitude of volume increase depending not only on the initial porosity, which is well known, but also on the pore water pressure increase rate: as the PPIR increased the dilational effect was increased. The effect of PPIR is similar to the effect of the initial porosity: dense sands dilate under shear, as do confined dense and loose sands under high PPIR.

[41] The results highlight the possible importance of the PPIR (especially under high rates) in controlling the volumetric response of dilative soils during the early stages of landslide deformation. Their influence is particularly important for soils in a dense condition, which exhibit a high sensitivity to pore water pressure rate changes.

[42] **Acknowledgments.** We thank K. Kondo for his technical assistance on arranging the triaxial apparatus to perform the pore water pressure controlled tests. The first author wishes to acknowledge the Ministry of Education, Culture, Sports, Science and Technology of Japan for its sponsorship. The authors are grateful to Kit-Ying (Angel) Ng, Alexander Edwards, and Domenico Gallipoli from Durham University for reviewing and commenting on the paper. Finally, the authors give special thanks to the Associate Editor and two reviewers of this paper, whose comments led to substantial improvement of this paper.

References

Anderson, S. A., and M. F. Riemer (1995), Collapse of saturated soil due to reduction in confinement, *J. Geotech. Geoenviron. Eng.*, *121*(2), 216–220.

Anderson, S. A., and N. Sitar (1995), Analysis of rainfall-induced debris flows, *J. Geotech. Geoenviron. Eng.*, *121*(7), 552–554.

Bishop, A. W., and D. J. Henkel (1964), *The Measurement of Soil Properties in the Triaxial Test*, 228 pp., Edward Arnold, London.

Bonte, M., P. Ergenzinger, and A. Rauen (2000), Geomorphological, hydrological and sedimentary control of an artificially induced debris flow, *Phys. Chem. Earth, Part B*, *25*, 745–749.

Brand, E. W. (1981), Some thoughts on rainfall induced slope failures, in *Proceedings of 10th International Conference on Soil Mechanics and Foundation Engineering*, pp. 373–376, A. A. Balkema, Brookfield, Vt.

Casagrande, A. (1936), Characteristics of cohesionless soils affecting the stability of slopes and earth fills, *J. Boston Soc. Civ. Eng.*, January , 13 – 32 . (Reprinted, *Contributions to Soil Mechanics*, *1925 to 1940*, pp. 257–276, Boston Soc. of Civ. Eng., Boston, Mass., 1940)

Castro, G. (1969), *Liquefaction of Sands*, *Harvard Soil Mech. Ser.*, vol. 8, Harvard Univ., Cambridge, Mass.

Chen, R., and S. Yang (2000), Study on debris-flow triggered by pore water pressure, in *Debris-Flow Hazards Mitigation: Mechanics, Prediction, and Assessment*, pp. 61–65, Am. Soc. of Civ. Eng., Reston, Va.

Chu, J., S. Leroueil, and W. K. Leong (2003), Unstable behavior of sand and its implication for slope instability, *Can. Geotech. J.*, *40*, 873–885.

Eckersley, J. D. (1986), The initiation and development of slope failures with particular reference to flowslides, Ph.D. dissertation, 264 pp., James Cook Univ., Townsville, Queensl., Australia.

Eckersley, J. D. (1990), Instrumented laboratory flowslides, *Geotechnique*, *40*, 489–502.

Ellen, S. D., and R. W. Fleming (1987), Mobilization of debris flows from soil slips, San Francisco Bay region, California, *Rev. Eng. Geol.*, *7*, 31–40.

Harp, E. L., W. G. Wells II, and J. G. Sarmiento (1990), Pore pressure response during failure in soils, *Geol. Soc. Am. Bull.*, *102*, 428–438.

Iverson, R. M. (1997), The physics of debris flows, *Rev. Geophys.*, *35*(3), 245–296.

Iverson, R. M., M. E. Reid, and R. G. LaHusen (1997), Debris-flow mobilization from landslides, *Annu. Rev. Earth Planet. Sci.*, *25*, 85–138.

Iverson, R. M., M. E. Reid, N. R. Iverson, R. G. LaHusen, M. Logan, J. E. Mann, and D. L. Brien (2000), Acute sensitivity of landslide rates to initial soil porosity, *Science*, *290*, 513–516.

Johnson, K. A., and N. Sitar (1990), Hydrologic conditions leading to debris-flow initiation, *Can. Geotech. J.*, *27*, 789–801.

Junaideen, S. M. (2005), Failure of saturated sandy soils due to increase in pore water pressure, Ph.D. dissertation, 236 pp., Univ. of Hong Kong, Hong Kong.

Lourenço, S. D. N., K. Sassa, and H. Fukuoka (2006), Failure process and hydrologic response of a two layer physical model: Implications for rainfall-induced landslides, *Geomorphology*, *73*, 115–130.

McDonnell, J. (1990), The influence of macropores on debris flow initiation, *Q. J. Eng. Geol.*, *23*, 325–331.

Mitchell, J. K. (1993), *Fundamentals of Soil Behavior*, 2nd ed., 437 pp., John Wiley, Hoboken, N. J.

Moriwaki, H., T. Inokuchi, T. Hattanji, K. Sassa, H. Ochiai, and G. Wang (2004), Failure processes in a full-scale landslide experiment using a rainfall simulator, *Landslides*, *1*, 277–288.

Nemat-Nasser, S., and N. Okada (2001), Radiographic and microscopic observation of shear bands in granular materials, *Geotechnique*, *51*, 753–765.

Ochiai, H., Y. Okada, G. Furuya, Y. Okura, T. Matsuri, T. Sammori, T. Terajima, and K. Sassa (2004), A fluidized landslide on a natural slope by artificial rainfall, *Landslides*, *1*, 211–219.

Poulos, S. (1981), The steady state of deformation, *J. Geotech. Eng. Div. Am. Soc. Civ. Eng.*, *107*, 553–562.

Reid, M. E. (1995), Slope instability caused by small variations in permeability, *J. Geotech. Geoenviron. Eng.*, *123*, 717–725.

Reid, M. E., R. G. LaHusen, and R. M. Iverson (2000), Debris-flow initiation experiments using diverse hydrologic triggers, in *Debris-Flow Hazards Mitigation: Mechanics, Prediction, and Assessment*, pp. 1–11, Am. Soc. of Civ. Eng., Reston, Va.

Vieira, B. C., and N. F. Fernandes (2004), Landslides in Rio de Janeiro: The role played by variations in soil permeability, *Hydrol. Processes*, *18*, 791–805.

Wang, G., and K. Sassa (2001), Factors affecting rainfall-induced flowslides in laboratory flume tests, *Geotechnique*, *51*, 587–599.

Wang, G., and K. Sassa (2003), Pore-pressure generation and movement of rainfall-induced landslides: Effects of grain size and fine particle content, *Eng. Geol.*, *69*, 109–125.

Zhu, J. H., and S. A. Anderson (1998), Determination of shear strength of Hawaiian residual soil subjected to rainfall-induced landslides, *Geotechnique*, *48*, 73–82.

H. Fukuoka, K. Sassa, and G. Wang, Disaster Prevention Research Institute, Kyoto University, Gokasho, Uji 611-0011, Kyoto, Japan. (wanggh@landslide.dpri.kyoto-u.ac.jp; sassa@scl.kyoto-u.ac.jp; fukuoka@landslide.dpri.kyoto-u.ac.jp)

S. D. N. Lourenço, School of Engineering, Durham University, South Road, Durham DH1 3LE, UK. (s.d.n.lourenco@durham.ac.uk)